Pegylated poly(anhydride) nanoparticles for oral delivery of docetaxel

Ruiz-Gatón, L., Espuelas, S., Larrañeta, E., Reviakine, I., Yate, L. A., & Irache, J. M. (2018). Pegylated poly(anhydride) nanoparticles for oral delivery of docetaxel. *European Journal of Pharmaceutical Sciences*, *118*, 165-175. https://doi.org/10.1016/j.ejps.2018.03.028

Published in:
European Journal of Pharmaceutical Sciences

Document Version:
Peer reviewed version

Queen's University Belfast - Research Portal:
Link to publication record in Queen's University Belfast Research Portal

Pegylated poly(anhydride) nanoparticles for oral delivery of docetaxel

Luisa Ruiz-Gatón[a,*], Socorro Espuelas[a], Eneko Larrañeta[a], Ilya Reviakine[b,#], Luis A. Yate[b,#] and Juan M. Irache[a,**]

[a] Nanomedicines and Vaccines (NANO-VAC) Research Group, University of Navarra, Pamplona, 31080, Spain.
[b] CIC biomaGUNE, San Sebastián, 20009, Spain

***Present address:**
CIDETEC Nanomedicine
Paseo Miramón 196
20009 – San Sebastián
Spain

****Corresponding author:**
Prof. Juan M. Irache
Nanomedicines and Vaccines (NANO-VAC) Research Group
Dep. Pharmacy and Pharmaceutical Technology
University of Navarra
C/ Irunlarrea, 1
31080 – Pamplona
Spain
Phone: +34948425600
Fax: +34948425619
E-mail: jmirache@unav.es

#These authors contributed to the XPS analysis

Abstract

The aim of this work was to investigate the potential of pegylated poly(anhydride) nanoparticles to enhance the oral bioavailability of docetaxel (DTX). Nanoparticles were prepared after the incubation between the copolymer of methyl vinyl ether and maleic anhydride (Gantrez® AN), poly(ethylene glycol) (PEG2000 or PEG6000) and docetaxel (DTX). The oral administration of a single dose of pegylated nanoparticles to mice provided sustained and prolonged therapeutic plasma levels of docetaxel for up 48-72 h. In addition, the relative oral bioavailability of docetaxel was around 32%. The organ distribution studies revealed that docetaxel underwent a similar distribution when orally administered encapsulated in nanoparticles as when intravenously as Taxotere®. This observation, with the fact that the clearance of docetaxel when loaded into the oral pegylated nanoparticles was found to be similar to that of intravenous formulation, suggests that docetaxel would be released at the epithelium surface and then absorbed to the circulation.

Key words: docetaxel, nanoparticles, pegylated, oral delivery; bioavailability

1. Introduction

Docetaxel (DTX) is a semisynthetic taxoid, analogue of paclitaxel, derived from the European yew tree (*Taxus bacata sp.*) and it is one of the most effective drugs in chemotherapy. It has proven to be useful against several types of cancers such as breast, ovarian, prostate, head and neck, gastric and non-small lung cancers [de Weger et al., 2014; Nieuweboer et al., 2015]. The mechanism of action of DTX, like other taxanes, is based on the stabilization of the microtubule dynamics and thereby disruption of the cell cycle [Nieuweboer et al., 2015]. This is due to its stronger binding capability to tubulin, docetaxel shows about 2 to 4 times more cytotoxicity effect on tumor cells than that of paclitaxel [Jones, 2006]. Docetaxel (Taxotere® and generics) is formulated as a concentrated aqueous solution containing polysorbate 80 (Tween® 80). The presence of this non-ionic surfactant has been related with severe side effects in some patients, including anaphylactic hipersensitivity reactions and cumulative fluid retention [Tang et al., 2016]. In order to minimize allergic reactions, patients require premedication with antihistamines (H_2) and corticosteroids [Kang et al., 2017]. Therefore, investigation of alternative intravenous formulations of docetaxel is underway, and several approaches based on conjugates with albumin [Esmaeili et al., 2009], nanoparticles [Cho et al., 2011; Hwang et al., 2008], liposomes [Deeken et al., 2013] and micelles [Dou et al., 2014] have been proposed.

Another possibility for docetaxel administration would be the use of the oral route. An important argument for docetaxel oral delivery is that this route of administration facilitates the implementation of chronic regimens and other dosing schedules such as metronomic therapies. This is particularly interesting for cell cycle specific agents and compounds with a predominant cytostatic effect (e.g. docetaxel) [Jiang et al., 2010; Wu et al., 2011]. Moreover,

oral chemotherapy can provide an easy way for the patients to take the drug by themselves at home, which will reduce their medical expenses and improve their quality of life.

Nevertheless, docetaxel has a poor oral bioavailability of about 8% in humans [Malingré et al., 2011] and less than 4% in rodents [Bardelmeijer et al., 2002]. The main reasons for this low and variable oral bioavailability of DTX are related to a high lipophilicity and a low permeability within the gut. In fact, docetaxel has poor aqueous solubility (4.93 μg/ml) and upon oral administration, intestinal uptake is seriously hampered by drug efflux through intestinal P-glycoprotein (P-gp) and systemic exposure is further limited by drug metabolism via cytochrome P450 (CYP) 3A [Kuppens et al., 2005; Malingré et al., 2001]. One of the most popular strategies to boost the oral bioavailability of docetaxel is the combination of an oral formulation of the taxane with inhibitors of both P-gp and CYP3A4. Therefore, different preclinical and clinical studies have demonstrated the validity of this idea based on the co-administration of the anticancer drug with cyclosporine A [Chiou et al., 2002] or ritonavir and elacridar [Hendrikx et al., 2014]. However, the use of drugs that inhibit these enzymes and transporters involves potential risks. In order to minimize these side effects other inhibitors such as curcumin [Yan et al., 2010] or flavonoids [Yang et al., 2011] have been proposed.

Another approach may be the use of pegylated poly(anhydride) nanoparticles. These nanoparticles based on the copolymer of methyl vinyl ether and maleic anhydride (Gantrez® AN), have demonstrated a good ability to improve the oral bioavailability of paclitaxel (up to 10 times, compared with “naked” nanoparticles) [Zabaleta et al., 2012; Calleja et al., 2014]. These results may be explained by the capability of PEG coatings to confer a high stability in digestive fluids minimizing the interaction of these nanoparticles with lumen contents [Tobio et al., 2000]. Similarly, the coating of nanoparticles with poly(ethylene glycol)s (PEGs) would

yield nanoparticles with slippery properties that facilitate the passage of these carriers through the mucus layer which is covering and protecting the intestinal epithelium [Yoncheva et al., 2005; Inchaurraga et al., 2015]. In addition, PEGs possess the disturbing capability on the effect of both the intestinal P-glycoprotein efflux pump [Hugger et al., 2002] and the cytochrome P450 [Johnson et al., 2002]. These activities may be of interest to promote the oral absorption of docetaxel.

Therefore, the aim of this work was the evaluation of the capability of pegylated poly(anhydride) nanoparticles as oral carriers for docetaxel. For this purpose, pegylated nanoparticles containing DTX were optimised and orally administered to Balb/c mice in order to study the pharmacokinetics and tissue distribution of this anticancer drug.

2. Materials and Methods

2.1. Materials

Docetaxel (USP 30, grade 99.0%) and paclitaxel (USP 28, grade >99.5%) were supplied by 21CECpharm (London, UK). Poly(methyl vinyl ether-co-maleic anhydride) or poly(anhydride) (PMV/MA) [Gantrez® AN 119; MW 200,000; density: 1.03 g/mL] was purchased from International Specialty Products ISP/Ahsland Inc. (KY, USA). Taxotere® from Sanofi-Aventis was provided by the Pharmacy Service of University Clinic of Navarra (Pamplona, Spain). Phosphate buffered saline (PBS), pancreatin and glycine were obtained from Sigma Aldrich (MO, USA). Poly(ethylene glycol) with MW of 2000 and 6000 Da (PEG2000 and PEG6000, respectively) and disodium edetate (EDTA) were provided by Fluka (Buchs, Switzerland). Pepsin, acetone, ethanol, t-buthylmethylether and acetonitrile were obtained from Merck (Darmstadt, Germany). Polysorbate 80 (Tween® 80) was supplied by Panreac (Barcelona, Spain). Deionised reagent water (18.2 MΩ resistivity) was prepared by a water purification

system (Wasserlab, Pamplona, Spain). The anaesthetic isoflurane (Isoflo®) was from laboratories Esteve (Barcelona, Spain). All others reagents and chemicals used were of analytical grade.

2.2. Preparation of poly(anhydride)nanoparticles

Docetaxel (DTX) was encapsulated in either conventional [Arbos et al., 2003] or pegylated poly(anhydride) nanoparticles. Pegylated nanoparticles with either PEG2000 or PEG6000 were prepared following the method published by Zabaleta et al. (2012) with minor modifications.

2.2.1. Docetaxel-loaded pegylated poly(anhydride) nanoparticles

Briefly, either PEG2000 or PEG6000 (12.5 mg) were firstly dispersed in 3 mL acetone and added to a solution of acetone containing 100 mg Gantrez® AN. The resulting mixture was maintained under magnetic agitation. On the other hand, docetaxel was dissolved in 0.5 mL acetone and added to the polymers mixture. Then, the organic phase containing DTX, PVM/MA and PEG was incubated for a period of 1 hour under magnetic stirring at room temperature. Afterwards, nanoparticles were formed by the addition of 20 mL of a hydroalcoholic solution (50% ethanol) containing glycine (0.5% w/v) and disodium edetate (0.18% w/v). The mixture was maintained under agitation for 10 minutes. The organic solvents were eliminated by evaporation under reduced pressure (Büchi Rotavapor® R-144; Büchi, Postfach, Switzerland) and the nanoparticle suspensions were purified by tangential filtration in Vivaspin tubes (Vivascience Sartorius, Hannover, Germany; MW cut off: 300,000) at 4,000 x*g* for 15 min. The pellets were resuspended in water and the purification step was repeated again. Finally, the formulations were frozen and freeze-dried (Genesis 12 EL Freeze Dryer; Virtis, PA, USA) using sucrose (5%) as cryoprotector. The resulting nanoparticles were identified as DTX-NP2 (docetaxel-loaded pegylated nanoparticles with PEG2000) and DTX-

NP6 (docetaxel-loaded pegylated nanoparticles with PEG6000).

Empty pegylated nanoparticles (NP2 and NP6) were prepared in the same way as described above but in absence of docetaxel and used as controls.

2.2.2. Docetaxel-loaded poly(anhydride) nanoparticles

Ten mg of docetaxel were incubated with 100 mg Gantrez® AN under magnetic stirring at room temperature for 1 hour in 5 mL acetone. Then, nanoparticles were formed by the addition of 20 mL of a mixture of ethanol and water (1:1 by vol.) containing glycine (0.5% w/v) and disodium edetate (0.18% w/v). The organic solvents were eliminated by evaporation under reduced pressure and the resulting nanoparticles were purified and freeze-dried as described above.

Empty poly(anhydride) nanoparticles (NP) were prepared in the same way but in the absence of docetaxel. For identification, the following abbreviations were used: NP, poly(anhydride) nanoparticles; DTX-NP, docetaxel-loaded poly(anhydride) nanoparticles.

2.3. Characterization of nanoparticles

2.3.1. Physico-chemical characterization

The mean hydrodynamic diameter of the nanoparticles and their zeta potential were determined by photon correlation spectroscopy (PCS) and electrophoretic laser Doppler anemometry, respectively, using a Zetamaster analyzer system (Malvern Instruments Ltd., Worcestershire, UK). The diameter of the nanoparticles was determined after dispersion in ultrapure water (1:10) and measured at 25°C by dynamic light scattering angle of 90°C. The zeta potential was determined as follows: 200 µL of the samples were diluted in 2 mL of a 0.1 mM KCl solution. The yield of the process was calculated by gravimetry as described previously [Arbos et al., 2003].

The morphological examination of the nanoparticles was carried out by field emission scanning electron microscopy (FESEM) and by energy-filtered transmission electron microscopy (EFTEM). For FESEM analysis, nanoparticles were washed before imaging by centrifugation to remove the cryoprotector. For this purpose, a small amount of the freeze-dried nanoparticles was resuspended in ultrapure water and centrifuged at 27,000x*g* for 10 min. Then, the supernatants were rejected and the obtained pellets were mounted on copper grids. FESEM was performed using a Zeiss ultra Plus electron microscopy (Carl Zeiss SMT, Oberdochen, Germany) operating between 1 a 2 Kv from 3 mm distance.

EFTEM was performed in a Zeiss Libra 120 (Carl Zeiss SMT, Oberkochen, Germany) operating at 80 kv. For this purpose, 20 µL of a suspension of nanoparticles were deposited onto copper grids for 1 min and excess suspension was blotted off using filter paper. Finally, samples were stained with phosphotungstic acid at 2% for 15 sec. The excess of this solution was blotted off using filter paper and grids were air dried before observation. Images were adquired using a 2k bottom-mount SlowScanCCD with YAG scintillator high-resolution camera (TRS-system, Moorenweis, Germany).

2.3.2. X-ray photoelectron spectroscopy (XPS)

Surface chemical composition of the nanoparticles was studied by X-ray photoelectron spectroscopy (XPS) in a SPECS SAGE HR 100 (SPECS, Berlin, Germany) spectrometer equipped with a Mg Kα (1253.6 eV) non-monochromatic source operated at 250 W. The take-off angle was fixed at 90º and the analyses were conducted at a pressure of ~10^{8} mbar. The pass energy was set at 30 and 15 eV for the general survey and the high resolution scans, respectively. The step size was 0.5 eV for the survey spectra and 0.1 for the high-resolution spectra, respectively. Charge compensation was achieved with an electron flood gun in the analysis chamber. The XPS data were processed with casaXPS V2.3.15 software

(Casa Software Ltd., Teignmouth, UK). Spectra were calibrated with the C-C peak position fixed at 285.0 eV [Moulder et al., 1992] after a Shirley background subtraction. The fitting procedure was done constraining the peak widths (same width for all peaks on each element) while the peak positions and areas were set free.

2.3.3. Quantification of the amounts of PEG associated with nanoparticles

The amount of PEG associated to the nanoparticles was determined by HPLC coupled to an evaporative light scattering detector (ELSD) [Inchaurraga et al., 2015], with minor modifications. Briefly, analysis was carried out in a model 1100 series Liquid Chromatography, Agilent (Waldbronn, Germany) coupled to an ELSD 2000 Alltech apparatus (Illinois, USA). Separation was carried out on a PL Aquagel-OH column (300 mm x 7.5 mm; particle size 5 µm) (Agilent, Wokingham, UK), in a gradient elution with methanol-water as mobile phase at a flow rate of 1 mL/min. ELSD conditions were set as follows: drift tube temperature was maintained at 110 ºC, nitrogen flow was set at 3 L/min and the gain was 1. For the quantification of PEG2000, ELSD conditions were modified as follows in order to achieve maximum sensitivity: the drift tube temperature was set at 90°C, the nitrogen flow was maintained at 3.2 L/min and the gain was set to 2.

For analysis, supernatants collected during the purification step of the preparative process were centrifuged at 17,000 rpm for 20 min at 4ºC. Then, aliquots of the supernatants (20 µL) were injected onto the HPLC column. The amount of PEG associated to nanoparticles was calculated as the difference between the initially added amount of PEG to the solution of the polymer in acetone and the amount of PEG recovered in the supernatants. Each sample was assayed in triplicate and the results were expressed as the amount of poly(ethylene glycol) per mg of nanoparticle.

2.3.4. Evaluation of the average PEG chain density and conformation state

The PEG surface density (d_{PEG}), the average distance between two neighbouring PEG chains (D) and the Flory Radius were calculated following the procedure described previously [Inchaurraga et al., 2015]. Then, the conformation state of PEG on the surface of nanoparticles was calculated by comparing D and RF. In any case, it was assumed that all the nanoparticles were spherical and displayed the same size (the mean size calculated by PCS). Similarly, it was also assumed that the associated PEG (as calculated by HPLC) was localized on the surface of the nanoparticles.

2.3.5. Docetaxel content in nanoparticles

The amount of docetaxel loaded in the nanoparticles was quantified by HPLC-UV. The analytical apparatus was an Agilent model 1200 series LC coupled to a diode-array detector (Agilent) set at 228 nm. The chromatographic system was equipped with a reversed-phase 150 mm x 3 mm C18 Phenomenex Gemini column (particle size 5 µm; Phenomenex, CA, USA) and protected by a 0.5 µm precolumn filter. The mobile phase, pumped at 0.5 mL/min, was a mixture of phosphate buffer (0.01 M; pH 2.1) and acetonitrile (50:50 v/v). The column was placed at 30°C and the injection volume was 100 µL. Paclitaxel (PTX) was used as internal standard. Under these experimental conditions the run time was 16 min and paclitaxel and docetaxel eluted at 6.8 and 8.2 min, respectively. For the calculations, the standard curve of docetaxel was designed over the range between 1.25 and 320 µg/mL (r^2>0.999). The limit of quantification was calculated as 60 ng/mL with a relative standard deviation of 4.5%.

For analysis, nanoparticles were digested with acetonitrile (1:8 volume ratio). Samples were transferred into auto-sampler vials, capped and placed in the HPLC auto-sampler. Each sample was assayed in triplicate and the results were expressed as the amount of docetaxel (µg) per mg of nanoparticles**.**

191 The encapsulation efficiency (E.E) was calculated as follows:

192 $$E.E.\ (\%) = (Q_{associated}/Q_{initial}) \times 100 \qquad (Eq.1)$$

193

194 Where $Q_{initial}$ is the initial amount of DTX added and $Q_{associated}$ is the amount of entrapped DTX

195 in the nanoparticles, which is calculated by HPLC.

196 **2.4. *In vitro* release study**

197 Release experiments were conducted, under sink conditions, at 37°C using simulated gastric

198 (SGF; pH 1.2; pepsin 0.32% w/v) and intestinal (SIF; pH 6.8; pancreatin 1% w/v) fluids

199 containing 0.5% of polysorbate 80 (Tween® 80) as solubilising agent for docetaxel. The

200 studies were performed under agitation in a Vortemp 56™ Shaking incubator (Labnet

201 International Inc., NJ, USA) after the dispersion of the nanoparticles in the appropriate

202 medium.

203 For each time point, 50 µg docetaxel formulated in nanoparticles were resuspended in 2 mL

204 of the corresponding simulated fluid. The concentration of the nanoparticles in the release

205 medium was adjusted in order to assess sink conditions for docetaxel. The different

206 formulations were kept in the SGF for 2 hours and for 14 hours in SIF. At different time

207 points, sample tubes were collected and centrifuged at 27,000x*g* for 20 minutes. Finally,

208 samples were filtered and the amount of docetaxel released from the formulations was

209 quantified by HPLC (calibration curves of free docetaxel in supernatants obtained from SGF

210 and SIF, r^2>0.999). Release profiles were expressed in terms of cumulative release

211 percentage, and plotted versus time.

212 **2.4.1. Analysis of release data**

213 Data obtained from the *in vitro* release experiments were treated by various conventional

214 mathematical models to determine the release mechanism of the drug from the

215 nanoparticles. Based on the highest regression values (r^2) for correlation coefficients for

formulations, the best-fit model was decided. For this purpose, the following models were used: the Korsmeyer-Peppas equation (Eq.2), the Higuchi equation (Eq.3), and zero-order equation (Eq.4).

The Korsmeyer-Peppas model exponentially relates drug release with the elapsed time [Ritger and Peppas, 1987]:

$$M_t/M_\infty = K_{KP} \times t^n \qquad \text{(Eq.2)}$$

In which M_t/M_∞ is the fraction of released drug at time *t*, K_{KP} is a constant incorporating the structural and geometric characteristics of the matrix, and n is the release exponent indicating the drug release mechanism. If "n" value is around 0.5 (the exact value depends on the geometry), the mechanism is Case I (Fickian) diffusion. A value between 0.5 and 0.89 indicates anomalous (non-Fickian) diffusion and a value of 0.89 and above indicates a Case II Transport.

When the release mechanism is mainly based on a Fickian diffusion, a dimensionless expression of the Higuchi model can be applied [Costa and Sousa, 2011]:

$$M_t/M_\infty = K_H \times t^{1/2} \qquad \text{(Eq.3)}$$

Where M_t/M_∞ is the fraction of released drug at time *t*, and K_H is the Higuchi constant.

Finally, the following zero-order kinetic model was also used. This model is used for systems where the matrix releases the same amount of drug by unit of time:

$$Q_t = Q_0 + K_{ZO} \times t \qquad \text{(Eq.4)}$$

Where Q_t is the amount of drug dissolved in time t and Q_0 is the initial amount of drug in the solution (most times, $Q_0 = 0$) and K_{ZO} is the zero-order release constant.

The analysis was applied to the release study of docetaxel performed under simulated intestinal fluid, until the 60-80% of drug released. All data processing was performed using Origin 8.0 software (OriginLab Corporation, MA, USA).

2.5. Pharmacokinetic studies

Pharmacokinetic studies were carried out in Balb/c female mice (average weight 19-22 g) obtained from Harlan (Santiga, Spain). Studies were approved by the Ethical Committee for Animal Experimentation of the University of Navarra (protocol number E21-12) in accordance with the European legislation on animal experiments (86/609/EU). Before the experiment, animals were adaptively fed for 1 week with free access to food and drinking water (22 ± 2°C; 12-h light and 12-h dark cycles; relative humidity 55 ± 10%). Previous to the oral administration of the formulations, animals were fasted overnight to avoid the interference with the absorption, allowing free access to water.

For the pharmacokinetic study, the animals were randomly divided into five groups. The experimental groups were as follows: (a) DTX-NP2, (b) DTX-NP6 and (c) DTX-NP. As controls, one group of animals received Taxotere® intravenously and another group was treated with the commercial formulation orally. Each animal received the equivalent amount of docetaxel to a dose of 30 mg/kg body weight (bw) either orally with a blunt needle via the esophagus into the stomach or intravenously via tail vein as a slow infusion. All the formulations were administered dispersed or dissolved in either purified water (oral) or sterile saline (intravenous). All animals were observed for their general condition and clinical signs.

At established times after administration, blood was obtained from 4 animals in each group. EDTA was used as an anticoagulant agent. Blood volume was recovered intraperitoneally with an equal volume of normal saline solution preheated at body temperature. Samples

were immediately placed on ice and centrifuged at 2,500x*g* for 10 minutes. Plasma was separated into clean tubes and kept frozen at -80ºC until HPLC analysis.

2.5.1. Determination of DTX plasma concentration by HPLC-UV

The amount of docetaxel was determined in plasma by HPLC-UV as described above. The extraction method was adapted from Zhao et al. (2010). Calibration curves were used for the conversion of the DTX/PTX chromatographic area to the concentration. Calibrator and quality control samples were prepared by adding appropriate volumes of standard docetaxel in ethanol to drug free plasma. Calibration curves were designed over the range between 100 and 3200 ng/mL (r^2>0.999). An aliquot (200 µL) of plasma was mixed with 25 µL of internal standard solution (paclitaxel, 10 µg/mL in ethanol). After vortex mixing, liquid–liquid extraction was accomplished by adding 3 mL of tert-buthylmethylether following vortex gentle agitation (10 min). The mixture was centrifuged for 10 min at 2,500x*g*, and then, the organic layer was transferred to a clean tube and evaporated to dryness (Thermo Savant, Barcelona, Spain). The residue was then dissolved in 125 µL of reconstitution solution (acetonitrile–phosphate buffer; 0.01 M; pH 2.1; 50:50 v/v) and transferred to auto-sampler vials, capped and placed in the HPLC auto-sampler. A hundred microlitre-aliquot of each sample was injected onto the HPLC column.

Under these experimental conditions the UV detection of docetaxel was performed at 228 nm and the run time was 16 min. The limit of quantification was calculated to be 140 ng/mL with a relative standard deviation of 5.3%. Accuracy values during the same day (intraday assay) at low, medium and high concentrations of docetaxel were always within the acceptable limits (less than 5%) at all concentrations tested.

2.5.2. Pharmacokinetic data analysis

The pharmacokinetic analysis of plasma concentration plotted against time data, obtained

from the administration of the different docetaxel formulations, was performed based on a non-compartmental model using WinNonlin 5.2 software (Pharsight Corporation, MO, USA). The following parameters were estimated: maximal plasmatic concentration (C_{max}), time in which the maximum concentration is reached (T_{max}), area under the concentration-time curve from time 0 to t h (AUC), mean residence time (MRT), clearance (Cl), volume of distribution (V) and half-life of the terminal phase ($t_{1/2z}$). In addition, the relative oral bioavailability (Fr) of docetaxel was calculated using the ratio of dose-normalized AUC values following oral and i.v. administrations:

$$Fr\ (\%) = AUC_{oral} / AUC_{i.v} \times 100 \qquad \text{(Eq.5)}$$

Where AUC_{oral} and $AUC_{i.v.}$ correspond to the areas under the plasma curve for the oral and intravenous (Taxotere®) administrations, respectively.

2.6. Organ distribution of docetaxel

To study the amount of anticancer drug in different organs after administration, animals received docetaxel loaded in the poly(anhydride) nanoparticles orally at a dose of 30 mg/kg. Treatment groups were DTX-NP, DTX-NP2 and DTX-NP6. In addition, a group of mice was treated intravenously with the commercial formulation, Taxotere®, at the same dose (30 mg/kg) as control. After administration, mice were sacrificed at different time points by cervical dislocation under isoflurane anesthesia (n=4 at each time point) and the following organs were harvested: liver, spleen, kidneys, lung, heart, stomach and intestine. In the group receiving the commercial formulation, animals were sacrificed at 4, 12 and 24 hours post-administration. The animals treated with the pegylated-poly(anhydride) nanoparticles (DTX-NP2 and DTX-NP6) were sacrificed at 8, 24 and 72 hours post-administration. Finally, for the DTX-NP group, the animals were killed at 8 h post-administration exclusively. Times points were selected based on the plasmatic curves obtained for the different formulations

in mice.

Each tissue simple was kept on ice, accurately weighted in polystyrene tubes and homogenized in 1 ml of PBS pH 7.4 using a Mini-bead beater (BioSpect Products Inc, OK, USA). Later, the homogenized organs were centrifuged at 10,000x*g* for 10 minutes. The supernatants were then collected and stored at -80°C until further analysis by the HPLC assay.

The amount of docetaxel in each tissue was determined by liquid-liquid extraction method followed by reverse-phase HPLC analysis. The method for the extraction was adapted from Zhao et al. (2010). Standardized calibration curves were used for each organ. As internal standard, paclitaxel was used and the conversion of the DTX/PTX chromatographic areas to concentration was performed.

For extractions, aliquots (200 µL) of the selected tissue samples were mixed with 25 µL PTX solution (10 µg/mL ethanol) for 1 min. Then, 3 ml t-buthylmethylether was added, and the resulting mixtures were vortex-mixing for 10 min. Next the mixture was centrifuged at 2,500x*g* for 10 min and the clear organic layer was transferred to a clean tube and evaporated until complete dryness. Finally, the residue was reconstituted with 125 µL of acetonitrile-phosphate buffer (0.01 M; pH 2.1; 50:50 v/v) and quantified by HPLC-UV.

2.7. Statistical analysis

Data are expressed as the mean ± S.D of at least three experiments. The non-parametric Kruskal-Wallis followed by U Mann-Whitney test was used to investigate statistical differences. In all cases, p values less than 0.05 were considered to be statistically significant. All calculations were performed using GraphPad Prism 6.0 statistical software (GraphPad Software, CA, USA).

3. Results

3.1. Preparation and characterization of poly(anhydride) nanoparticles

Table 1 summarizes the main physico-chemical properties of the different poly(anhydride) nanoparticles used in this work. Overall, pegylation of DTX-loaded nanoparticles slightly decreased the mean size (220 nm for conventional and about 200 nm for pegylated nanoparticles) and the negative zeta potential of the resulting nanoparticles (-43 mV *vs*. -35 mV). Besides, the polydispersity index (PDI) was lower than 0.2 and the yield of the process was calculated to be between 60 and 65%. Empty nanoparticles displayed similar physico-chemical characteristics than the DTX-loaded ones except for the yield of the process which was slightly higher than in the presence of the anticancer drug (between 70 and 80%). Similarly the mean size of empty nanoparticles was found to be slightly smaller than in the presence of docetaxel (see Table 1).

In addition, the amounts of PEG associated with the poly(anhydride) nanoparticles were quantified by HPLC-ELSD. The analysis revealed that the amount of PEGs associated to nanoparticles was significantly higher when nanoparticles were pegylated with PEG6000 (~55 µg/mg) than with PEG2000 (~40 µg/mg) ($p<0.05$). Based on these calculations, the estimated values of PEG densities on the surface of nanoparticles decreased with increasing the length of the PEG chain. Thus, d_{PEG} was about 3-times higher for nanoparticles pegylated with PEG2000 than when PEG6000 (0.46 *vs.* 0.15 nm^{-2}). On the other hand, as for both types of nanoparticles D was smaller than the Flory Radius (data not shown), the PEG chains adopted a “brush” conformation on the surface of both pegylated nanocarriers.

Regarding the amount of docetaxel loaded in the nanoparticles, the addition of glycine to conventional nanoparticles enhanced dramatically the docetaxel loading, making it 20-times higher than when conventional nanoparticles were prepared in absence of this amino acid

(data not shown). For conventional nanoparticles, docetaxel content was estimated in 60 μg DTX/mg NP. However, for pegylated nanoparticles (DTX-NP2 and DTX-NP6), the docetaxel payload significantly increased. Thus, for nanoparticles pegylated with PEG6000 the DTX content was around 90 μg DTX/mg NP, whereas for DTX-NP2 the drug loading was almost 2-times higher than for "nacked" nanoparticles (approx. 111 μg/mg NP). The encapsulation efficiency for DTX-NP2 and DTX-NP6 nanoparticles was 60 and 78%, respectively, whereas for DTX-NP it was about 42%.

Figure 1 shows the microphotographs obtained by field emission scanning and energy-filtered transmission electron microscopy of the nanoparticles. In all cases, the apparent sizes of nanoparticles were similar to the values obtained by photon correlation spectroscopy. All the nanoparticles formulations displayed spherical shapes. Moreover, conventional nanoparticles presented a smooth or plain surface (Figure 1A) whereas pegylated ones appeared to show a spongy and diffuse surface (Figures 1B and 1C). In addition, from EFTEM analysis (Figure 1D), pegylated nanoparticles appeared as spherical structures surrounded by a long and diffuse dark area.

X-ray photoelectron spectroscopy (XPS) technique quantified the elemental and average chemical composition by measuring the binding energy of electrons associated with atoms around 5-10 nm depth inside the polymeric surface. Fittings of the C1s spectra (atomic orbital 1s of carbon) of the surface of the poly(anhydride) nanoparticles and its components were examined (Table 2). Comparing the different control nanoparticles (NP, NP2 and NP6), when PEG was incorporated to the formulation, the content of C-O bonds progressively increased from NP (11%) to NP2 (19%) and NP6 (21%) while the proportion of C=O and C-C/C-H bonds decreased. For the docetaxel-loaded formulations (DTX-NP, DTX-NP2 and DTX-NP6), the addition of PEG induced a decrease of the signal related to the presence of C=O

383 bonds (15% for DTX-NP and 8% for DTX-NP6). In parallel, pegylation of nanoparticles
384 produced an important increase on the percentage of C-O bond values and a decrease of the
385 C-C/C-H intensity (Table 2).
386 Regarding the surface elemental composition (in atomic percentage values) of the samples,
387 the carbon and oxygen content was very similar in all control formulations (NP, NP2 and
388 NP6). However, the nitrogen signal is only detected in loaded-DTX nanoparticles (DTX-NP,
389 DTX-NP2 and DTX-NP6). Thus, the nitrogen content progressively decreased when PEG was
390 added to these loaded formulations while the oxygen content increased.

391 **3.2. *In vitro* release study**

392 Figure 2 depicts the release profiles of docetaxel from the different formulations expressed
393 as cumulative percentage of drug released as a function of time. In all cases, when
394 nanoparticles were incubated in SGF, no drug release was observed. In contrast, when
395 nanoparticles were dispersed in the SIF, docetaxel was released. For DTX-NP2 the release
396 pattern in SIF was characterized by an important burst effect of about 75% of the loaded
397 drug in the first 30 min followed by a more sustained deliverance phase up to 10 hours. On
398 the other hand, for DTX-NP and DTX-NP6, the release curves of docetaxel in SIF exhibited a
399 slower discharge of docetaxel than DTX-NP2 followed by a more steady release up to the
400 end of the study in which almost all of their cargo was extracted. In any case, 1 h after the
401 incubation of nanoparticles in SIF, the amount of docetaxel released from DTX-NP6 was
402 about 65% of the loaded drug whereas for DTX-NP, only 55% of the drug was released.
403 The release profiles of DTX from nanoparticles were evaluated by fitting the *in vitro* data into
404 various kinetic models (Table 3). For DTX-NP and DTX-NP2, the experimental data of the
405 docetaxel release in SIF fitted well into the Korsmeyer-Peppas equation (Eq.2) with
406 regression coefficients higher than 0.98. For both nanoparticle formulations, the release

exponent (n) was calculated to be lower than 0.5. For DTX-NP6, the data were adequately adjusted to the three models. The obtained r^2 values for these models were around 0.8. However, the calculated "n" value in the Korsmeyer-Peppas equation, was about 0.8 (Table 3).

3.3. Pharmacokinetic studies

The plasma concentration-time profile of docetaxel after iv administration of Taxotere® (single dose of 30 mg/Kg) to female Balb/c mice is shown in Figure 3. The drug plasma concentration rapidly decreased in a biphasic way with time and data were adjusted to a non-compartmental model. Levels of docetaxel in plasma were quantifiable until 12 hours post-administration. The estimated AUC was 140 µg h/ml with a maximum concentration (C_{max}) of 198 µg/mL. The mean residence time (MRT) and the half-life of the terminal phase ($t_{1/2z}$) were estimated to be 1.5 hours. The clearance (Cl) of docetaxel was 0.2 L/h/kg and the volume of distribution (V) of the drug was about 0.5 L/kg (Table 4).

Figure 4 shows the plasma concentration versus time profiles after oral administration of docetaxel (single dose of 30 mg/kg) to Balb/c mice when administered as commercial Taxotere® or encapsulated in the different poly(anhydride) nanoparticle formulations. When Taxotere® was orally administered to mice, docetaxel plasma levels were found to be always below the quantification limit of the chromatographic analytical technique. On the contrary, when docetaxel was loaded in nanoparticles, these formulations displayed sustained plasma levels. In all cases, there was an initial rapid rise in the anticancer plasma levels for the first 2 hours, reaching the C_{max}, this was followed by a slow decline which was prolonged for at least 8 hours for DTX-NP, and about 70 hours for the PEG containing formulations (DTX-NP2 and DTX-NP6). Comparing DTX-NP2 with DTX-NP6, DTX-NP2 provided slightly higher levels of the anticancer drug than those determined for DTX-NP6. Another important fact to highlight

was that, for both nanoparticle formulations, the docetaxel plasma levels were within the therapeutic window. For docetaxel, in rodents, this therapeutic window would be between 35 ng/mL (minimum effective dose) and 2700 ng/mL (maximum tolerated dose) [Mei et al., 2013].

Table 4 summarizes the pharmacokinetic parameters calculated with a non-compartmental analysis of the experimental data obtained after the administration of the different docetaxel formulations to mice. For DTX-NP2 and DTX-NP6, AUC values were respectively 6.5 and 5-fold higher than the AUC obtained for non-pegylated nanoparticles (DTX-NP), demonstrating a higher capability to promote the oral absorption of the taxane. In addition, C_{max} values of docetaxel in the poly(anhydride) nanoparticles was between 1.3 and 2 µg/ml. The rank order of this parameter was DTX-NP6 > DTX-NP2 > DTX-NP. Moreover, the C_{max} was reached at 0.08 h for DTX-NP,1.5-2 h for DTX-NP6 and DTX-NP2. Furthermore, the mean residence time (MRT) of the drug in plasma and the half-life of the terminal phase ($t_{1/2z}$) were found to be similar for pegylated nanoparticles (both DTX-NP2 and DTX-NP6). Interestingly, for all the formulations and routes of administration tested, the clearance of docetaxel displayed a similar value (about 0.2 L/h/kg). On the contrary, the volumen of distribution (V) of the anticancer drug was about 10 times higher when loaded in pegylated nanoparticles than for DTX-NP and Taxotere® intravenously administered. Finally, the relative oral bioavailability of docetaxel delivered in pegylated nanoparticles was calculated to be around 24% for DTX-NP6 and 32% DTX-NP2. For control nanoparticles, the oral bioavailability was found to be of about 5%.

3.4. Organ distribution of docetaxel

Organ distribution of docetaxel was evaluated in Balb/c mice after the administration of a single dose (30 mg/kg) either intravenously as Taxotere® or orally after encapsulation in

455 nanoparticles. Figure 5 summarises the levels of the anticancer drug in the different organs
456 at different times after administration. For i.v. Taxotere®, the highest concentration of
457 docetaxel 4 h post-administration was found in the spleen (about 31 µg DTX/g tissue) and
458 the liver (about 24 µg DTX/g tissue). Also, an important and similar amount of drug was
459 quantified in the kidneys, lung and heart (about 16-18 µg DTX/g tissue). These levels
460 decreased rapidly with time and 24 h post-administration only significant amounts of
461 docetaxel were quantified in spleen (about 10 µg DTX/g tissue).
462 For DTX-NP2 and DTX-NP6 orally administered, the amount of the drug recovered in the
463 different organs of animals was similar for both formulations. Thus, 24 hours after
464 administration, docetaxel was mainly found in spleen and liver (~20 µg DTX/g tissue),
465 followed by intestine (~18 µg DTX/g tissue), lung and kidneys (~13 µg DTX /g tissue). As time
466 increased, the drug amounts in tissues decreased, even so, 72 hours post-administration
467 significant amounts of docetaxel were still quantified in the spleen, lung and kidneys (about
468 5 µg DTX /g tissue).
469 Figure 6 represents the amount of docetaxel recovered in different organs of animals 8 h
470 after the administration of a single dose of the anticancer drug (30 mg/kg) formulated in
471 nanoparticles or as Taxotere®. Overall, 8 h post-administration the amounts of anticancer
472 drug found in the liver, lungs and gut for pegylated nanoparticles (DTX-NP2 and DTX-NP6),
473 were higher than for Taxotere®. Thus, the liver of animals treated with docetaxel orally as
474 pegylated nanoparticles displayed 3-times more drug than when intravenously administered
475 as Taxotere®. By contrast, 8 h post-administration, the levels of docetaxel when
476 administered in conventional nanoparticles (DTX-NP) were dramatically low, close to the
477 quantification limit of the HPLC technique (280 ng/mL).
478 Focusing on the differences observed amongst nanoparticles, there were not significant

differences between DTX-NP2 and DTX-NP6 for all the organs tested.

4. Discussion

The oral bioavailability of taxanes (e.g. docetaxel) is hampered by both their high lipophilic character and low permeability related to their affinity to the P-glycoprotein and cytochrome P450 enzymatic complex [Wu et al., 2011; Malingré et al., 2001]. In order to solve these problems and thus enhance the oral absorption of these drugs, one possible solution may be the encapsulation of these drugs into polymeric nanoparticles with both mucus-penetrating properties and inhibitory abilities of the efflux pump activity and cythocrome P450 metabolism. The pegylation of nanoparticles from the copolymer of methyl vinyl ether and maleic anhydride yields submicronic carriers with these capabilities [Yoncheva et al., 2005; Inchaurraga et al., 2015]. In addition, acute and sub-acute toxicity studies in rats clearly demonstrated the absence of toxic or side effects when these nanoparticles were orally administered [Ojer et al., 2012]. In the present work, our aim was to gain more insight about the structure and composition of these pegylated nanoparticles as well as explore their potential as oral delivery systems for docetaxel.

Pegylation of poly(anhydride) nanoparticles slightly decreased the mean size and the negative zeta potential of “naked” nanoparticles (Table 1). Furthermore, the amount of PEG associated to the nanoparticles was significantly higher when nanoparticles were pegylated with PEG6000 than with PEG2000. This observation is in line with previous reported data [Zabaleta et al., 2012; Inchaurraga et al., 2015], in which it was described a higher degree of pegylation by increasing the MW of the PEG. All PEG-coated nanoparticles used have their PEG chains in a “brush” conformation, independent of the PEG chain molecular weight.

Regarding the encapsulation of docetaxel in nanoparticles, glycine and EDTA were employed to increase its loading into the resulting nanoparticles. Thus, when the amino acid and the chelating agent was added to the medium in which the nanoparticles were obtained, the drug loading was about 20-30 times higher than in the absence of both auxiliary excipients (about 3 μg/mg nanoparticles). The chelating agent would prevent the opening of the anhydride groups by the presence of bivalent cations, whereas glycine would promote the encapsulation of docetaxel in the resulting nanoparticles. In fact, the addition of glycine would alter the solvent properties of the mixture in which the nanoparticles are formed, decreasing the solubility of the polymer in this medium and facilitating the interaction between the polymer and docetaxel by hydrophobic bonds. A similar effect has been observed by adding glycine to different kinds of micelles, generating important increases of their capability to load hydrophobic compounds (i.e., quercetin) [Ruiz et al., 2008; Pillai et al., 2016].

On the other hand, the docetaxel loading was also found to be dependent on both the presence and MW of PEG employed for pegylation. In this way, the use of PEG2000 allowed us to increase almost 2-times the docetaxel payload compared to “naked” nanoparticles. These results agree well with previous studies with PLGA/PLA particles [Enolw et al., 2011], which reported a significant increase of docetaxel loading in pegylated PLGA/PLA delivery systems, in comparison with the conventional ones, due to the solubilising properties of PEG. In addition, PEG2000 appeared to be slightly superior for increasing the docetaxel entrapment in poly(anhydride) nanoparticles.

From the observations by electronic microscopy techniques (Figure 1), these pegylated nanocarriers would adopt a structure based on a solid core surrounded by a PEG corona. In order to study this structure, the surface of nanoparticles was examinated by XPS analysis

(Table 2). Comparing “naked” nanoparticles (NP) with pegylated ones (NP2 and NP6), the percentage of C-O bonds, which are typical in the poly(ethylene glycol) structure [Baer and Engelhard, 2010], increased after nanoparticle pegylation. In addition, NP6 produced a slightly more intense signal of C-C/C-H bonds than NP2. This observation would be related to a longer C-C/C-H chain for PEG6000 than for PEG2000. When docetaxel was loaded into “naked” nanoparticles (DTX-NP), an increase in the XPS signals related with the presence of C-N bonds was found. This fact would be due to the presence of both the anticancer drug and glycine. Additionally, the presence of docetaxel and glycine also induces a reduction in the percentages of C-C/C-H and C=O bonds, as compared with NP. For pegylated nanoparticles, the presence of PEG at the surface of nanoparticles would hinder the access and, therefore, the binding of glycine to the surface of nanoparticles. In the case of DTX-NP2, this finding would be supported by a decrease of the nitrogen content for these nanoparticles (as compared with DTX-NP) as well as by the decrease in the percentage of C-N/C-O bonds that can be attributed to the substitution of glycine by PEG. Finally, for DTX-NP6, elemental analysis displayed a very low amount of nitrogen associated with a high content of oxygen. In addition, these nanoparticles showed a low percentage of C=O and C-C/C-H bonds and a quite high content of C-N/C-O bonds. These last observations would be related to the presence of the PEG chains at the surface of nanoparticles. To sum up, the reduction of the nitrogen content would be associated to the presence of PEG in the samples. In addition, the presence of longer PEG chains would be reflected by an increase in the percentage of C-N/C-O bonds. Moreover, the decrease in the percentage of C=O bonds (typical for anhydride residues) observed for pegylated nanoparticles (mainly for those pegylated with PEG 6000) would be directly related to the particular characteristics of the XPS technique, which is adapted to the investigation of the surface properties of a given

material [Baer and Engelhard, 2010]. All together would probe that pegylation of these poly(anhydride) nanoparticles yields a PEG coating.

Docetaxel release profiles from nanoparticle formulations were evaluated in simulated gastric and intestinal fluids, both containing Tween 80 as solubilising agent. In all cases, no drug release was observed when nanoparticles were incubated in acid conditions. However, under simulated intestinal pH conditions, docetaxel was rapidly released with small differences between “naked” and pegylated nanoparticles. Thus, pegylated nanoparticles displayed profiles characterized by an initial release pulse of 65-75% of the loaded drug followed by a slow deliverance phase of the remaining drug. For DTX-NP, the curve was characterized by an initial burst effect of about 40% followed by a sustained and continuous release step. Interestingly, the release pulse was almost immediate for DTX-NP2 formulation whereas, for nanoparticles pegylated with PEG6000 the burst effect only appeared after 1 h of incubation in SIF. Analysis of the release data also highlighted a different behaviour between nanoparticle formulations. The release of docetaxel from DTX-NP and DTX-NP2, characterised by a Korsmeyer-Peppas exponent coefficient lower than 0.5, would be explained by a quasi-Fickian Higuchi diffusion mechanism, typical of matrix-type devices. On the contrary, the mechanism involved in the release of docetaxel from DTX-NP6 (with a Korsmeyer-Peppas coefficient of 0.8) would be a combination between diffusion and erosion. In this case, the presence of long chains of poly(ethylene glycol) at the surface of the nanoparticles would hamper the diffusion of the loaded drug. So the release of the loaded drug will be delayed until the nanoparticle matrix will start to be eroded/dissolved.

For the pharmacokinetic study in mice, a single dose of 30 mg docetaxel per kg bw was selected. Taxotere®, intravenously administered, presented a characteristic nonlinear profile (Figure 3) that has been previously reported by other authors [Nieuweboer et al., 2015; Van

574 Tellingen et al., 1999] and associated with the effect of micellar entrapment on DTX in
575 presence of Tween® 80 in the formulation, which could affect the distribution of unbound
576 drug [Nassar et al., 2011; Desai et al., 2008]. At the administered dose, the plasmatic levels
577 of docetaxel diminished rapidly, and 12 hours post-administration, no levels of the drug
578 were quantified. The non-linearity was caused mainly during the first hours after drug
579 administration when the concentrations were relatively high. From this curve, the mean AUC
580 and the half-life of the terminal phase ($t_{1/2z}$) for docetaxel were estimated to be about 140
581 µg h/ mL and 1.5 hours, respectively. The volume of distribution (V) was 0.5 L/h and
582 clearance (Cl) was 0.2 L/h/kg. These results are consistent with data previously published by
583 Van Tellingen et al. (1999), who administered Taxotere® at similar dose level (33 mg
584 docetaxel per kg bw) in female FVB mice. In contrast, when commercial Taxotere® was
585 administered orally, the drug plasma levels were below the quantification limit of our
586 technique. In any case, the oral bioavailability of docetaxel in mice has been previously
587 reported to be around 3.6% [Bardelmeijer et al., 2002].
588 When docetaxel was orally administered after encapsulation in pegylated nanoparticles, the
589 plasma levels of the anticancer drug were high and sustained in time till 3 days. For “naked”
590 nanoparticles, the docetaxel plasma concentration was initially high but decreased rapidly
591 and no quantifiable levels were found 12 h after administration. More importantly, the
592 docetaxel plasma levels provided by pegylated nanoparticles were found to be within the
593 therapeutic window [Saremi et al., 2011; Mei et al., 2013]. This observation is particularly
594 interesting for an oral docetaxel treatment that would permit to achieve long-term drug
595 exposure and predicted responses [Bruno et al., 1998]. Moreover, the half-life of the drug
596 was greatly extended from 1.5 h for intravenous administration to 35 h for oral
597 administration of pegylated nanoparticles (Table 4). This may be due to the capability of

598 pegylated nanoparticles to reach the surface of the enterocyte, therefore prolonging their
599 residence at the site of absorption. Another important fact was that the metabolism of
600 docetaxel appeared to be not affected when it was carried by the nanoparticles ($p<0.01$). In
601 fact, the clearance of docetaxel from DTX-NP and pegylated nanoparticles was similar to the
602 value calculated from the i.v. administration of Taxotere®. Compared to DTX-NP, pegylated
603 nanoparticles increased the drug elimination half-life, mean residence time (MRT) and
604 volume of distribution (V) (Table 4). These results would corroborate that when docetaxel is
605 loaded into pegylated nanoparticles, the drug has sustained release, prolonged half-life and
606 increased tissue appetency. As a consequence, the relative oral bioavailability obtained for
607 the different pegylated nanoparticles were high, varying from 24 to 33% for DTX-NP6 and
608 DTX-NP2 respectively. These bioavailability results are slightly higher than others reported
609 previously using solid lipid nanoparticles [Cho et al., 2014] or self-nano-emulsifying drug
610 delivery systems [Seo et al., 2013]. Nevertheless, the bioavailability of docetaxel in pegylated
611 nanoparticles was lower than the value reported by Feng et al. (2009) with poly(lactide)-
612 vitamin E TPGS/montmorillonite nanoparticles on SD rats (about 90%).
613 The distribution of the orally administered docetaxel, when loaded into pegylated
614 nanoparticles, appeared to be quite similar to that elicited by Taxotere® (Figures 5 and 6).
615 The comparative evaluation of the drug levels in different organs was quite similar for both
616 intravenous Taxotere® and pegylated nanoparticles; although this similar trend was delayed
617 in time for the oral treatments. In both cases, docetaxel accumulates in the liver, spleen,
618 lungs, intestine and kidneys. The main difference, if any, is the decreased levels of docetaxel
619 observed in the hearts of animals treated orally with pegylated nanoparticles (Figure 6).
620 All together these results suggest that pegylated nanoparticles, after reaching the surface of
621 the enterocytes, would release the loaded docetaxel and, in parallel, disturb the effect of P-

622 gp and cytochrome P450. Obviously, the possibility that these pegylated nanoparticles
623 penetrate the enterocytes cannot be discarded; although their absorption through the blood
624 and/or lymphatic routes would be unlikely. This idea would be supported by the similar
625 elimination (clearance) and distribution of docetaxel in vivo from pegylated nanoparticles
626 and intravenous Taxotere®. Another factor supporting this explanation would be that these
627 pegylated nanoparticles when incubated with Caco-2 cells were not capable to be
628 internalized [Ojer et al., 2013]. In line with this, biodistribution studies of these pegylated
629 nanoparticles (radiolabelled with technetium-99m) demonstrated that the localization of
630 these carriers after oral administration was restricted to the gut [Ojer et al., 2012]. It is also
631 important to take into account that the drug plasma levels are in line with the intestinal cell
632 renewal cycle, which takes 3–5 days [Barker, 2014]. Furthermore, in an aqueous medium at
633 neutral/basic pH, the anhydride residues of the polymer used to prepare our nanoparticles
634 (Gantrez® AN) suffer from hydrolysis yielding carboxylic groups. Under these conditions, the
635 ionization of these –COOH groups would induce a swelling of the nanoparticle shell
636 facilitating the drug release and hampering its entry into the cells. In any case, the behaviour
637 of pegylated nanoparticles would be different to that proposed for PLGA nanocapsules
638 [Attili-Qadri et al., 2013] or solid lipid nanoparticles [Cho et al., 2014]. In these cases, these
639 nanodevices would penetrate into the enterocytes and move into the circulation via the
640 lymphatic system [Attili-Qadri et al., 2013]. Probably, the lipid character of the oily core of
641 these nanoparticles would favour this particular behaviour.
642 In summary, pegylated nanoparticles provide an adequate device for the oral delivery of
643 docetaxel. When orally administered, these nanoparticles offered prolonged and sustained
644 plasma levels of the anticancer drug for 3 days. In addition, the relative oral bioavailability
645 was calculated to be up to 32% and between 5 and 6-times higher than for “naked”

nanoparticles. Interestingly, the elimination and distribution of docetaxel in vivo from pegylated nanoparticles and intravenous Taxotere® was found to be similar, suggesting that these nanoparticles would remain within the gut after reaching the surface of the enterocytes and would not enter into the circulation.

Acknowledgements

This work was supported by grants from "Caja de Ahorros de Navarra" (CAN) project "Nanotecnología y medicamentos" (ref 10828) and by the Spanish Ministry of Science and Innovation (project SAF2008-02538). Luisa Ruiz-Gatón was also financially supported by a grant from "Friends Association of the University of Navarra".

Disclosures section

Portions of this manuscript were presented and published in thesis form (Pegylated nanoparticles to falicitate the intravenous-to-oral switch in docetaxel cancer chemotherapy) in fulfillment of the requirements for the PhD for Student Miss Luisa Ruiz-Gatón from University of Navarra.

The authors declare no conflict of interest.

References

Arbos, P., Wirth, M., Arangoa, M.A., Gabor, F., Irache, J.M., 2003. Gantrez® AN as a new polymer for the preparation of ligand–nanoparticle conjugates. J. Control. Release. 83, 321-330.

Attili-Qadri, S., Karra, N., Nemirovski, A., Schwob, O., Talmon, Y., Nassar, T., et al., 2013. Oral delivery system prolongs blood circulation of docetaxel nanocapsules via lymphatic

absorption. Proc. Natl. Acad. Sci. USA. 110, 17498-17503.

Baer, D.R., Engelhard, M.H., 2010. XPS analysis of nanostructured materials and biological surfaces. J. Electron Spectrosc. Relat. Phenom. 178-179, 415-432.

Bardelmeijer, H.A., Ouwehand, M., Buckle, T., Huisman, M.T., Schellens, J.H., Beijnen, J.H., et al., 2002. Low systemic exposure of oral docetaxel in mice resulting from extensive first-pass metabolism is boosted by ritonavir. Cancer Res. 62, 6158-6164.

Barker, N., 2014. Adult intestinal stem cells: critical drivers of epithelial homeostasis and regeneration, Nat Rev Mol Cell Biol 15 (2014) 19-33.

Bruno, R., Hille, D., Riva, A., Vivier, N., ten Bokkel Huinnink, W.W., van Oosterom, A.T., et al., 1998. Population pharmacokinetics/pharmacodynamics of docetaxel in phase II studies in patients with cancer. J. Clin. Oncol. 16, 187-196.

Calleja, P., Espuelas, S., Corrales, L., Pio, R., Irache, J.M., 2014. Pharmacokinetics and antitumor efficacy of paclitaxel-cyclodextrin complexes loaded in mucus-penetrating nanoparticles for oral administration. Nanomedicine. 9, 2109-2021.

Chiou, W.L., Wu, T.C., Jeong, H.Y., 2002. Enhanced oral bioavailability of docetaxel by coadministration of cyclosporine: quantitation and role of P-glycoprotein. J. Clin. Oncol. 20, 1951-1952.

Cho, H.J., Park, J.W., Yoon, I.S., Kim, D.D., 2014. Surface-modified solid lipid nanoparticles for oral delivery of docetaxel: enhanced intestinal absorption and lymphatic uptake. Int. J. Nanomed. 13, 495-504.

Cho, H.J., Yoon, H.Y., Koo, H., Ko, S.H., Shim, J.S., Lee, J.H., et al., 2011. Self-assembled nanoparticles based on hyaluronic acid-ceramide (HA-CE) and Pluronic® for tumor-targeted delivery of docetaxel. Biomaterials. 32, 1781-1790.

693 Costa, P., Sousa, J.M., 2011. Modeling and comparison of dissolution profiles. Eur. J. Pharm.
694 Sci. 13, 123-133.
695 de Weger, V.A., Beijnen, J.H., Schellens, J.H., 2014. Cellular and clinical pharmacology of the
696 taxanes docetaxel and paclitaxel--a review. Anticancer Drugs. 25, 488-494.
697 Deeken, J.F., Slack, R., Weiss, G.J., Ramanathan, R.K., Pishvaian, M.J., Hwang, J., et al., 2013.
698 A phase I study of liposomal-encapsulated docetaxel (LE-DT) in patients with advanced solid
699 tumor malignancies. Cancer Chemother. Pharmacol. 71, 627-633.
700 Desai, N.P., Trieu, V., Hwang, L.Y., Wu, R., Soon-Shiong, P., Gradishar, W.J., 2008. Improved
701 effectiveness of nanoparticle albumin-bound (nab) paclitaxel versus polysorbate-based
702 docetaxel in multiple xenografts as a function of HER2 and SPARC status. Anticancer Drugs.
703 19, 899-909.
704 Dou, J., Zahng, H., Xiuju, L., Zhang, M., Zhai, G., 2014. Preparation and evaluation in vitro and
705 in vivo of docetaxel loaded mixed micelles for oral administration. Colloids Surf. B
706 Biointerfaces. 114, 20-27.
707 Enolw, E.M., Luft, J.C., Napier, M.E., De Simone, J.M., 2011. Potent engineered PLGA
708 nanoparticles by virtue of exceptionally high chemotherapeutic loadings. Nano Letters. 11,
709 808-813.
710 Esmaeili, F., Dinarvand, R., Ghahremani, M.H., Amini, M., Rouhani, H., Sepehri, N., et al.,
711 2009. Docetaxel-albumin conjugates: preparation, in vitro evaluation and biodistribution
712 studies. J. Pharm. Sci. 98, 2718-2730.
713 Feng, S.S., Mei, L., Anitha, P., Gan, C.W., Zhou, W., 2009. Poly(lactide)-vitamin E
714 derivate/montmorillonite nanoparticle formulations for the oral delivery of docetaxel.
715 Biomaterials. 30, 3297-3306.

716 Hendrikx, J.J., Lagas, J.S., Wagenaar, E., Rosing, H., Schellens, J.H., Beijnen, J.H., et al., 2014.
717 Oral co-administration of elacridar and ritonavir enhances plasma levels of oral paclitaxel
718 and docetaxel without affecting relative brain accumulation. Br. J. Cancer. 27, 2669-2676.
719 Hugger, E.D., Audus, K.L., Borchardt, R.T., 2002. Effects of poly(ethylene glycol) on efflux
720 transporter activity in Caco-2 cell monolayers. J. Pharm. Sci. 91, 1980-1990.
721 Hwang, H.Y., Kim, I.S., Kwon, I.C., Kim, Y.H., 2008. Tumor targetability and antitumor effect
722 of docetaxel-loaded hydrophobically modified glycol chitosan nanoparticles. J. Control.
723 Release. 18, 23-31.
724 Inchaurraga, L., Martín-Arbella, N., Zabaleta, V., Quincoces, G., Peñuelas, I., Irache, J.M.,
725 2015. In vivo study of the mucus-permeating properties of PEG-coated nanoparticles
726 following oral administration. Eur. J. Pharm. Biopharm. 97, 280-289.
727 Jiang, H., Tao, W., Zhang, M., Pan, S., Kanwar, J.R., Sun, X., 2010. Low-dose metronomic
728 paclitaxel chemotherapy suppresses breast tumors and metastases in mice. Cancer Invest.
729 28, 74-84.
730 Johnson, B.M., Charman, W.N., Porter, C.J., 2002. An in vitro examination of the impact of
731 polyethylene glycol 400, Pluronic P85, and vitamin E d-alpha-tocopheryl polyethylene glycol
732 1000 succinate on P-glycoprotein efflux and enterocyte-based metabolism in excised rat
733 intestine. AAPS PharmSciTech. 4, 193-205.
734 Jones, S., 2006. Head-to-Head: docetaxel challenges paclitaxel. Eur. J. Cancer Suppl. 4, 4-8.
735 Kang, R.Y., Yoo, K.S., Han, H.J., Lee, J.Y., Lee, S.H., Kim, D.W., et al., 2017. Evaluation of the
736 effects and adverse drug reactions of low-dose dexamethasone premedication with weekly
737 docetaxel. Support Care Cancer. 25, 429-437.
738 Kuppens, I.E., Bosch, T.M., van Maanen, M.J., Rosing, H., Fitzpatrick, A., Beijnen, J.H., et al.,
739 2005. Oral bioavailability of docetaxel in combination with OC144-093 (ONT-093). Cancer

740 Chemother. Pharmacol. 55, 72-78.
741 Malingré, M.M., Beijnen, J.H., Schellens, J.H., 2001. Oral delivery of taxanes. Invest. New
742 Drugs. 19, 155-162.
743 Mei, L., Zhang, Z., Zhao, L., Huang, L., Yang, X.L., Tang, J., et al., 2013. Pharmaceutical
744 nanotechnology for oral delivery of anticancer drugs. Adv. Drug Deliv. Rev. 65, 880-890.
745 Moulder, J.F., Stickle, W.F., Sobol, P.E., Bomben, K.D., Chastain, J., 1992. Handbook of X-ray
746 Photoelectron Spectroscopy, Perkin-Elmer Corporation Physical Electronics Division, Eden
747 Prairie, MN.
748 Nassar, T., Attili-Qadri, S., Harush-Frenkel, O., Farber, S., Lecht, S., Lazarovici, P., et al., 2011.
749 High plasma levels and effective lymphatic uptake of docetaxel in an orally available
750 nanotransporter formulation. Cancer Res. 71, 3018-3028.
751 Nieuweboer, A.J., de Morrée, E.S., de Graan, A.J., Sparreboom, A., de Wit, R., Mathijssen,
752 R.H., 2015. Inter-patient variability in docetaxel pharmacokinetics: a review. Cancer Treat.
753 Rev. 41, 605-613.
754 Ojer, P., de Cerain, A.L., Areses, P., Peñuelas, I., Irache, J.M., 2012. Toxicity studies of
755 poly(anhydride) nanoparticles as carriers for oral drug delivery. Pharm. Res. 29, 2615-2627.
756 Ojer, P., Neutsch, L., Gabor, F., Irache, J.M., de Cerain, A.L., 2013. Cytotoxicity and cell
757 interaction studies of bioadhesive poly(anhydride) nanoparticles for oral antigen/drug
758 delivery. J. Biomed. Nanotechnol. 9, 1891-1903.
759 Pillai, S.A., Bharatiya, B., Casas, M., Lage, E.V., Sandez-Macho, I., Pal, H., et al., 2016. A
760 multitechnique approach on adsorption, self-assembly and quercetin solubilization by
761 Tetronics® micelles in aqueous solutions modulated by glycine. Colloids Surf. B:
762 Biointerfaces. 148, 411–421.

763 Ritger, P.L., Peppas, N.A., 1987. A simple equation for description of solute release I. Fickian
764 and non-fickian release from non-swellable devices in the form of slabs, spheres, cylinders or
765 discs. J. Control. Release. 5, 23–36.
766 Ruiz, C.C., Hierrezuelo, J., Molina-Bolívar, J., 2008. Effect of glycine on the surface activity
767 and micellar properties of N-decanoyl-N-methylglucamide. Colloid Polym. Sci. 286, 1281–
768 1289.
769 Saremi, S., Dinarvand, R., Kebriaeezadeh, A., Ostad, S.N., Atyabi, F., 2011. Enhanced oral
770 delivery of docetaxel using thiolated chitosan nanoparticles: preparation, in vitro and in vivo
771 studies, Int. J. Nanomed. 6, 119-128.
772 Seo, Y.G., Kim, D.H., Ramasamy, T., Kim, J.H., Marasini, N., Oh, Y.K., et al., 2013.
773 Development of docetaxel-loaded solid self-nanoemulsifying drug delivery system (SNEDDS)
774 for enhanced chemotherapeutic effect. Int. J. Pharm. 452, 412-420.
775 Tang, X., Wang, G., Shi, R., Jiang, K., Meng, L., Ren, H., et al., 2016. Enhanced tolerance and
776 antitumor efficacy by docetaxel-loaded albumin nanoparticles. Drug Deliv. 23, 2686-2696.
777 Tobío, M., Sánchez, A., Vila, A., Soriano, I.I., Evora, C., Vila-Jato, J.L., Alonso, M.J., 2000. The
778 role of PEG on the stability in digestive fluids and in vivo fate of PEG-PLA nanoparticles
779 following oral administration. Colloids Surf. B Biointerfaces. 18, 315-323.
780 Van Tellingen, O., Beijnen, J.H., Verweij, J., Scherrenburg, E.J., Nooijen, W.J., Sparreboom, A.,
781 1999. Rapid esterase-sensitive breakdown of polysorbate 80 and its impact on the plasma
782 pharmacokinetics of docetaxel and metabolites in mice. Clin. Cancer Res. 5, 2918-2924.
783 Wu, H., Xin, Y., Zhao, J., Sun, D., Li, W., Hu, Y., et al., 2011. Metronomic docetaxel
784 chemotherapy inhibits angiogenesis and tumor growth in a gastric cancer model. Cancer
785 Chemother. Pharmacol. 68, 879-887.

786 Yan, Y.D., Kim, D.H., Sung, J.H., Yong, C.S., Choi, H.G., 2010. Enhanced oral bioavailability of
787 docetaxel in rats by four consecutive days of pre-treatment with curcumin. Int. J. Pharm.
788 399, 116-120.
789 Yang, S.H., Lee, J.H., Lee, D.Y., Lee, M.G., Lyuk, K.C., Kim, S.H., 2011. Effects of morin on the
790 pharmacokinetics of docetaxel in rats with 7,12-dimethylbenz[a]anthracene (DMBA)-induced
791 mammary tumors. Arch. Pharm. Res. 34, 1729-1734.
792 Yoncheva, K., Lizarraga, E., Irache, J.M., 2005. Pegylated nanoparticles based on poly(methyl
793 vinyl ether-co-maleic anhydride): preparation and evaluation of their bioadhesive properties.
794 Eur. J. Pharm. Sci. 24, 411-419.
795 Zabaleta, V., Ponchel, G., Salman, H., Agueros, M., Vauthier, C., Irache, J.M., 2012. Oral
796 administration of paclitaxel with pegylated poly(anhydride) nanoparticles: Permeability and
797 pharmacokinetic study. Eur. J. Pharm. Biopharm. 81, 514-523.
798 Zhao, M., Su, M., Lin, X., Luo, Y., He, H., Cai, C., et al., 2010. Evaluation of docetaxel
799 intravenous lipid emulsion: pharmacokinetics, tissue distribution, antitumor activity, safety
800 and toxicity. Pharm. Res. 27, 1687-1702.
801
802

Figure Legends

Figure 1. Field emission scanning electron microscopy (FESEM) and energy-filtered transmision electron microscopy (EFTEM) images of the different poly(anhydride) nanoparticles loaded with docetaxel. FESEM image of DTX-NP (A), DTX-NP6 (B) and DTX-NP2 (C). EFTEM image of DTX-NP2 (D).

Figure 2. Docetaxel release profiles from the poly(anhydride) nanoparticles formulations after incubation in simulated gastric fluid (SGF) and simulated intestinal fluid (SIF) at 37°C. Data represented as mean ± S.D. (n=4).

Figure 3. Docetaxel plasma concentration-time profile after a single intravenous dose in Balb/c mice (30 mg/kg) dose of the commercially available formulation Taxotere®. Data are expressed as mean ± S.D., n=4 per time point.

Figure 4. Docetaxel plasma levels as a function of time after the oral administration of nanoparticle formulations as a single dose of 30 mg/kg bw in Balb/c mice. Data are expressed as mean ± S.D., n=4 per time point.

Figure 5. Organ distribution time profiles of docetaxel in Balb/c mice after i.v. administration of Taxotere® (A) or oral administration of docetaxel loaded in pegylated nanoparticles with either PEG2000 (B) or PEG6000 (C). All mice received a single dose of 30 mg/kg. Data are expressed as mean ± S.D. (n=4).

Figure 6. Comparative organ distribution of docetaxel following the oral administration of the different poly(anhydride) nanoparticles loaded with docetaxel and the intravenous administration of Taxotere® at 8 hours after administration in Balb/c mice. All mice received a single dose of 30 mg/kg. Data are expressed as mean ± S.D. (n=4). *$p<0.05$ Taxotere® vs. nanoparticle formulations: DTX-NP, DTX-NP2 and DTX-NP6.

Figure(s) 1
Click here to download high resolution image

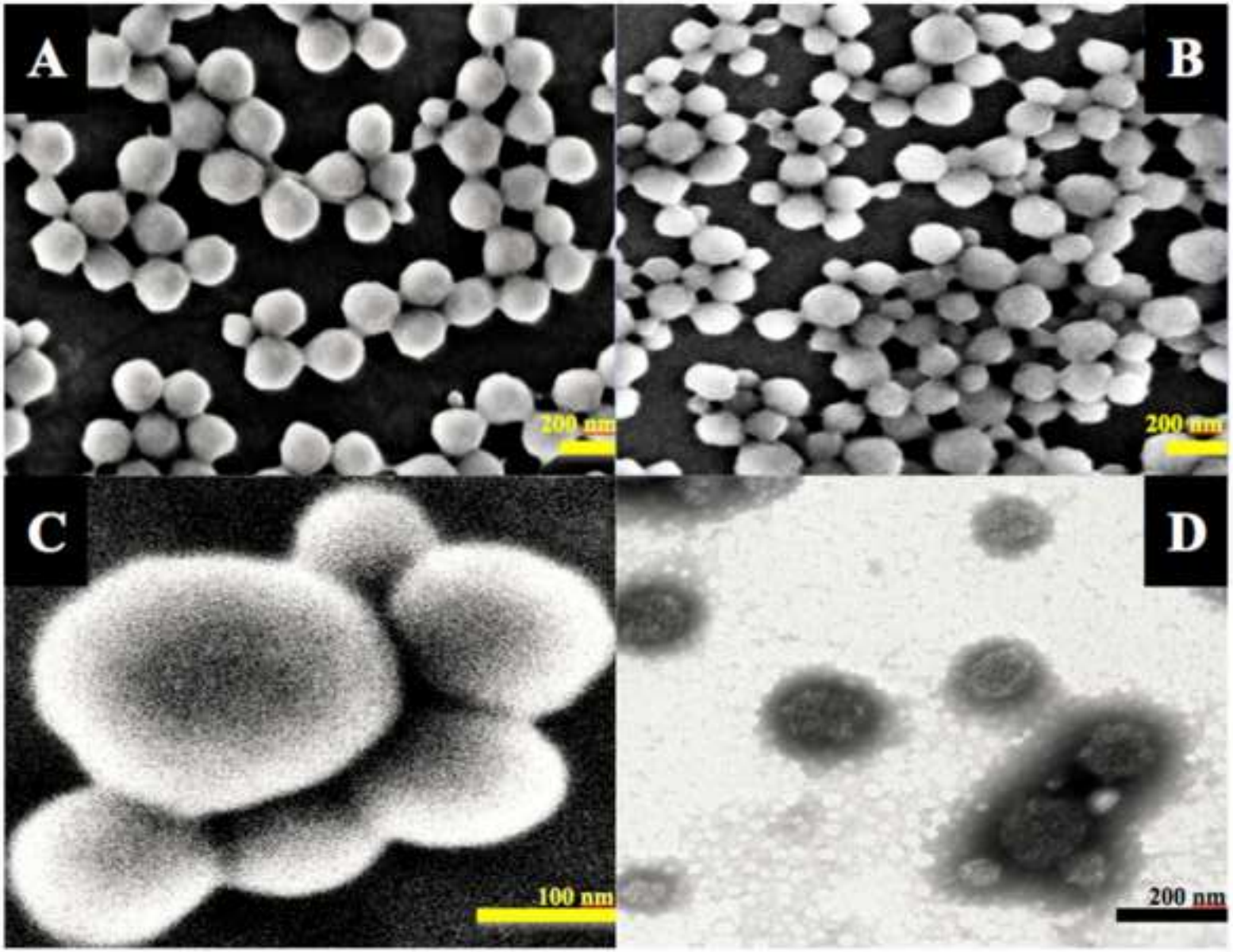

Figure(s) 2

Click here to download high resolution image

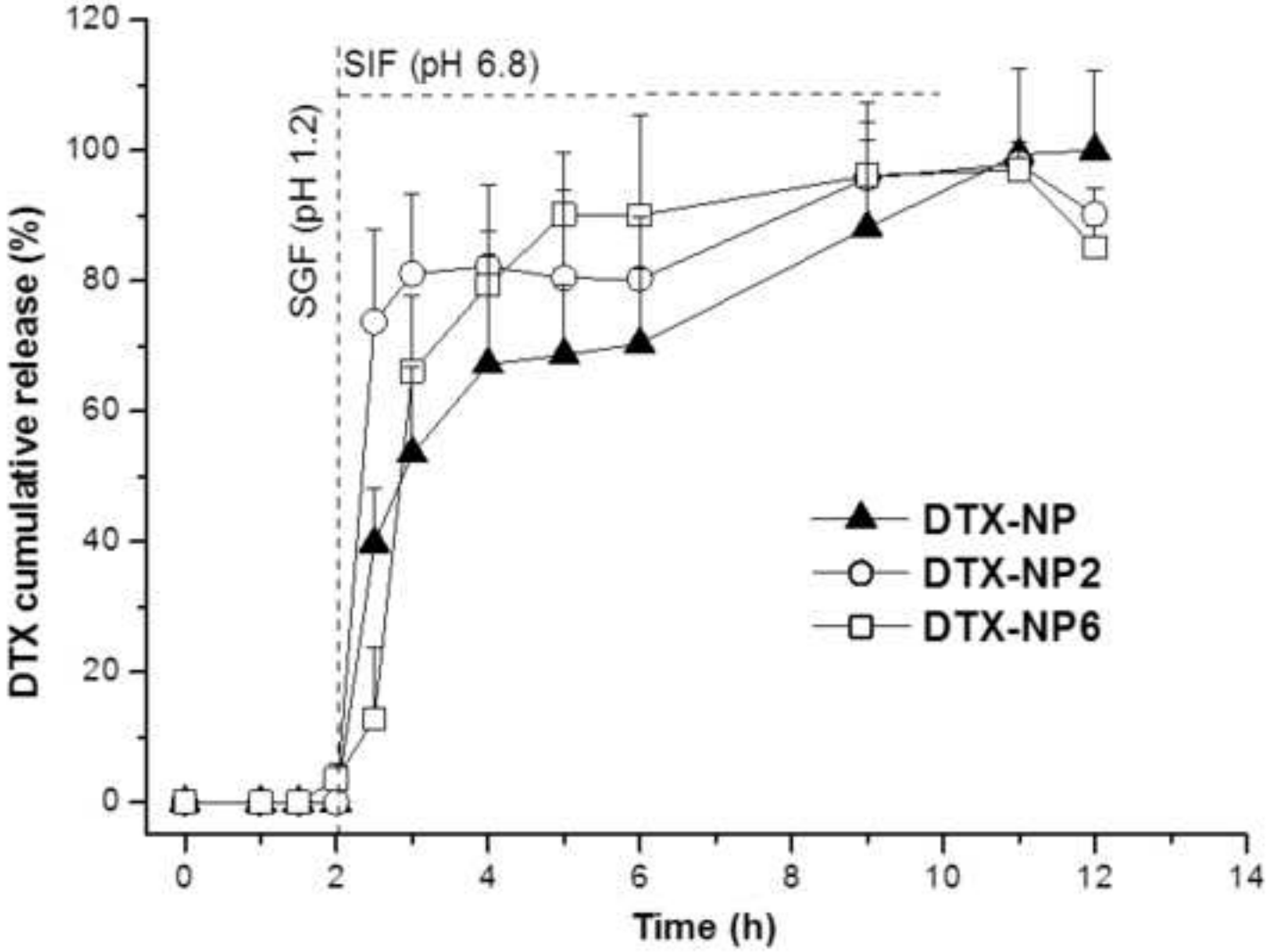

Figure(s) 3
Click here to download high resolution image

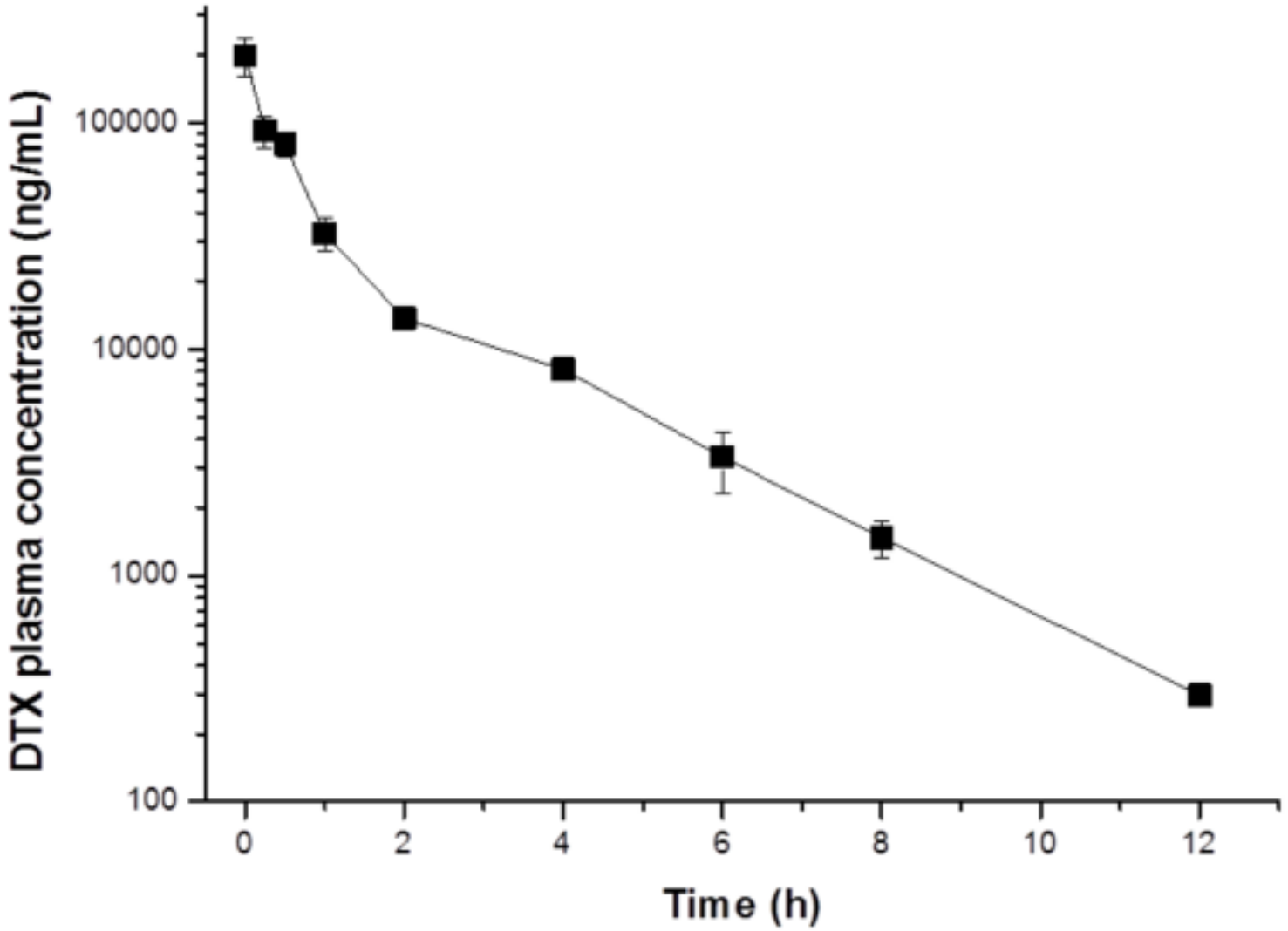

Figure(s) 4

Click here to download high resolution image

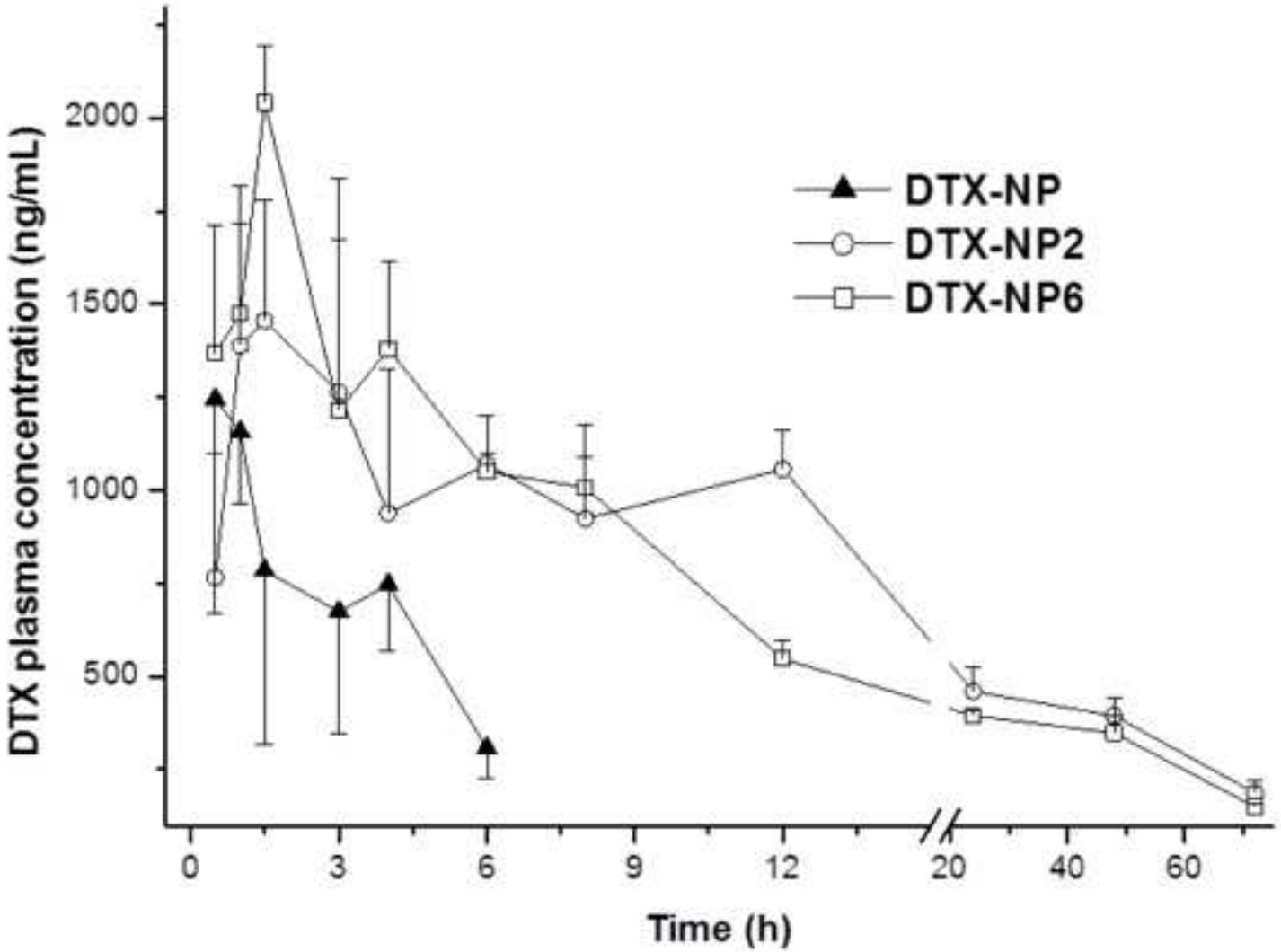

Figure(s) 5

Click here to download high resolution image

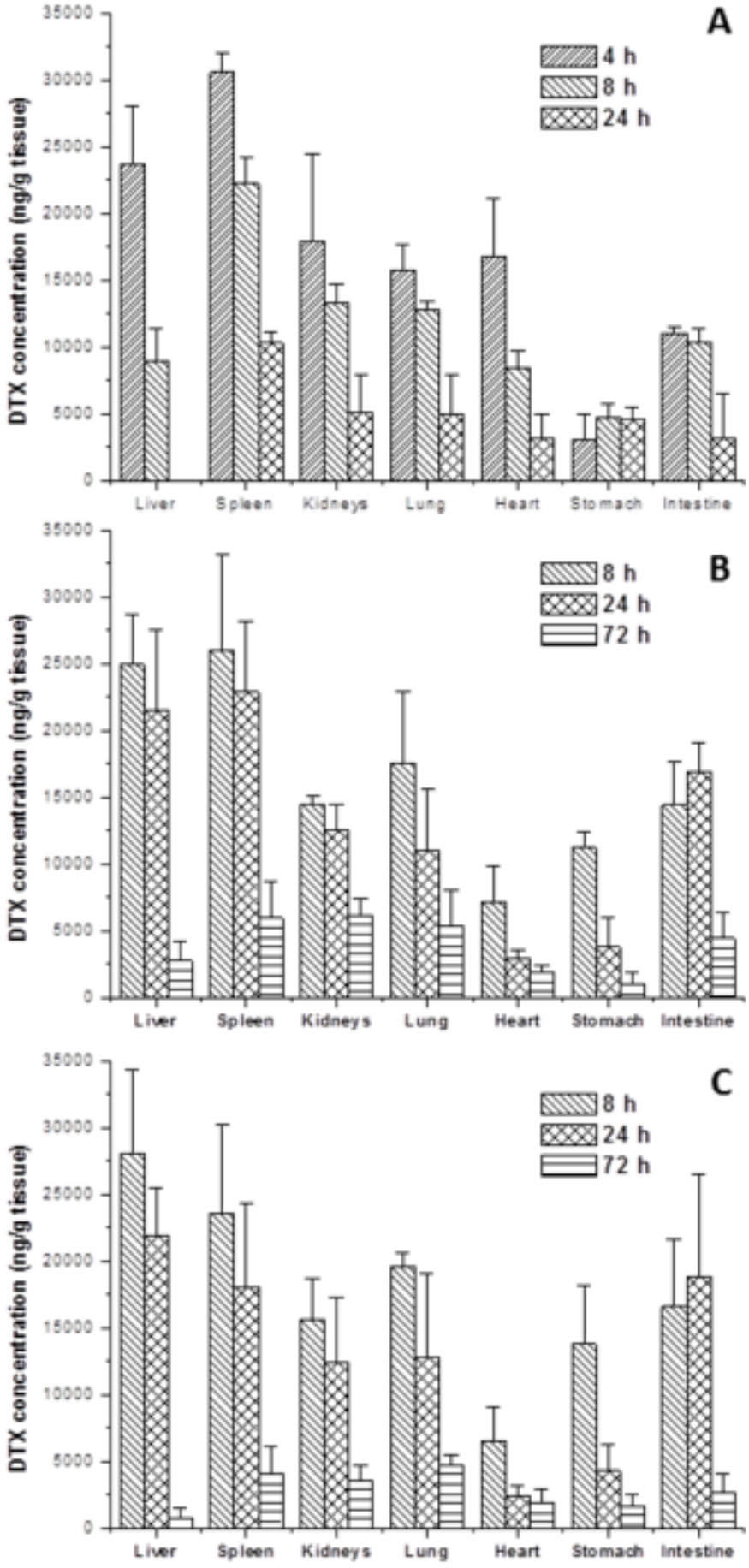

Figure(s) 6
Click here to download high resolution image

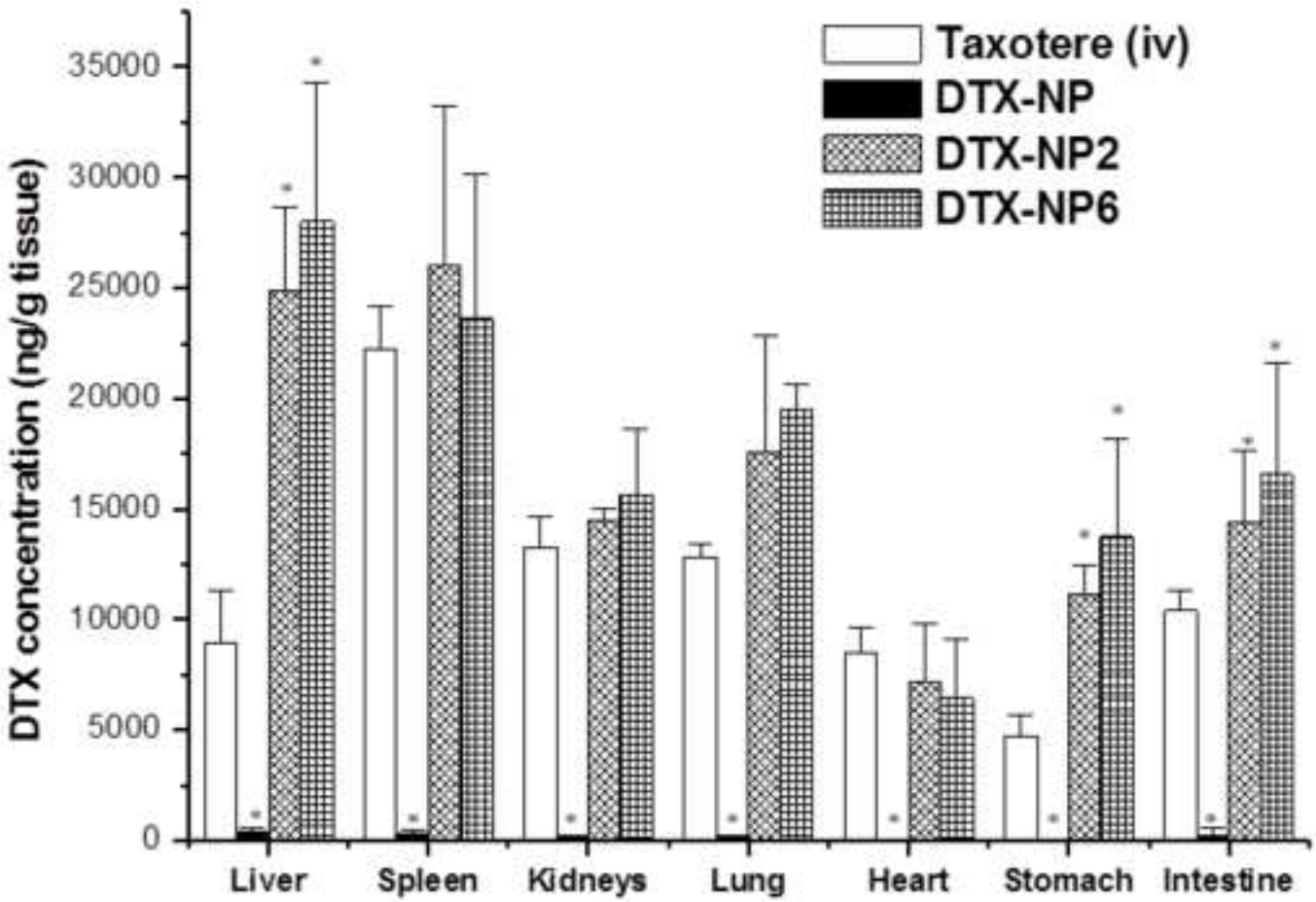

Table 1. Physico-chemical characterization of the poly(anhydride) nanoparticles obtained. Data are expressed as mean±S.D. (n=4). NP: control nanoparticles; NP2: control pegylated nanoparticles with PEG2000; NP6: control pegylated nanoparticles with PEG6000; DTX-NP: docetaxel-loaded nanoparticles; DTX-NP2: docetaxel-loaded in pegylated nanoparticles with PEG2000; DTX-NP6: docetaxel-loaded in pegylated nanoparticles with PEG6000.

	Size (nm)	**Zeta Potential (mV)**	**PDI**	**Yield (%)**	**PEG content (µg/mg)**	**DTX loading (µg/mg)**	**EE (%)**
NP	167±2	-55±6	0.07	79±3	-	-	-
DTX-NP	220±2	-43±1	0.15	65±3	-	60±2	42±4
NP2	154±3	-42±3	0.05	72±3	36.2±3.1†	-	-
DTX-NP2	203±4	-36±4	0.07	62±3	43.8±6.1†	111±3*†	78±9*†
NP6	157±2	-45±4	0.07	68±1	54.1±2.2	-	-
DTX-NP6	197±3	-33±2	0.08	60±5	56.7±1.9	88±2*	60±2*

*p<0.05 Mann Whitney U-test DTX-NP2 vs. DTX-NP, DTX-NP6 vs. DTX-NP; † p<0.05 Mann Whitney U-test DTX-NP2 vs. DTX-NP6, NP2 vs. NP6.

Table 2. Elemental ratio of the elements and fitting results of the C1s peak of nanoparticle formulations. The C-O/C-N components are shown together because they present the same position in the C1s spectra (around 286.5 eV) and it is not possible to resolve them individually.

Formulation	XPS elemental ratio (%)			XPS C1s fitting ratio (%)		
	C	O	N	C = O	C-O / C-N	C-C / C-H
NP	68	32	0	16	11	42
NP2	68	32	0	14	19	35
NP6	71	29	0	15	21	36
DTX -NP	69	28	3	15	21	33
DTX-NP2	67	31	2	14	16	37
DTX-NP6	58	41	1	8	36	14

Table 3. Kinetic parameters of *in vitro* release profiles of DTX-loaded nanoparticles. Data are expressed as mean ± S.D. (n=4).

Formulation	Korsmeyer-Peppas			Higuchi		Zero-order	
	K_{KP} (h^{-n})	n	r^2	K_H ($h^{-1/2}$)	r^2	Kz (h^{-1})	r^2
DTX-NP	0.52±0.02	0.25±0.04	0.98	0.42±0.03	0.87	0.23±0.04	0.28
DTX-NP2	0.79±0.01	0.10±0.02	0.99	0.72±0.11	0.79	0.5±0.2	0.24
DTX-NP6	0.4±0.1	0.8±0.4	0.78	0.53±0.09	0.81	0.44±0.06	0.85

Table 4. Pharmacokinetic parameters of docetaxel in female Balb/c mice for the different formulations tested. Dose DTX= 30 mg/kg.

Data are expressed as mean ± S.D. (n=4).

Formulation	Route	AUC (μg h/ mL)	C_{max} (μg/ mL)	T_{max} (h)	MRT (h)	$T_{½ z}$ (h)	Cl (L/h/kg)	V (L/kg)	Fr (%)
Taxotere®	i.v	142.6 ± 1.9	197.9 ± 37.2	0.08	1.4 ± 0.1	1.5 ± 0.1	0.2 ± 0.1	0.5 ± 0.2	100
Taxotere®	p.o	N.D	N.D	N.D	N.D	N.D	N.D	N.D	N.D
DTX-NP	p.o	6.9 ± 1.6*	1.3 ± 0.4	0.8	4.2 ± 0.2*	2.2 ± 0.3*	0.2 ± 0.1	0.8 ± 0.1*	4.9
DTX-NP2	p.o	45.9 ± 3.5*†	1.5 ± 0.3	2	43.5 ± 9.8*†	34.7 ± 9.6*†	0.2 ± 0.1	9.6 ± 0.7*†	32.2
DTX-NP6	p.o	33.8 ± 1.2*†	2.0 ± 0.2	1.5	41.7 ± 2.3*†	34.6 ± 2.5*†	0.2 ± 0.1	8.6 ± 0.7*†	23.7

AUC: Area under the concentration-time curve from time 0 to t h; C_{max}: Peak plasma concentration; T_{max}: Time to reach peak plasma concentration; $t_{1/2\ z}$: Half-life of the terminal phase; Cl: Clearance; V: Volume of distribution; MRT: Mean residence time; Fr: relative oral bioavailability. *p<0.05 Mann-Whitney U-test DTX-NP vs. Taxotere® i.v., DTX-NP2 vs. Taxotere® i.v., DTX-NP6 vs. Taxotere® i.v..† p<0.05 Mann Whitney U-test DTX-NP2 vs. DTX-NP, DTX-NP6 vs. DTX-NP.